

## Search for Short-Lived Particles Produced in an Electron Beam Dump

A. Bross, M. Crisler, S. Pordes, and J. Volk

*Fermi National Accelerator Laboratory, Batavia, Illinois 60510*

S. Errede and J. Wrbanek<sup>(a)</sup>

*University of Illinois, Urbana, Illinois 61801*

(Received 12 July 1991)

A search for short-lived neutral particles which decay to electron-positron pairs has been carried out using a beam of 275-GeV electrons incident on an instrumented tungsten beam dump. The experiment was sensitive to particles up to  $10 \text{ MeV}/c^2$  in mass and down to  $4 \times 10^{-16}$  sec in lifetime.

PACS numbers: 14.80.Gt, 13.60.Hb

Monoenergetic positron peaks seen in heavy-ion collision experiments [1] at the Gesellschaft für Schwerionenforschung (GSI) have been interpreted as a signal for the production and subsequent decay into an electron-positron pair of a new neutral boson  $X_0$  with mass about  $1.8 \text{ MeV}/c^2$  [2]. This suggestion was supported by the observation of coincident electron-positron pairs having equal laboratory energies ( $E_{e^+} + E_{e^-} = 1.8 \text{ MeV}/c^2 - 2m_e$ ) [3]. Although simple models for a neutral  $X_0$  are constrained by limits obtained from precision atomic physics experiments [4,5] and by null results from previous searches in nuclear decay [6], in beam-dump experiments [7-9] and in low-energy Bhabha scattering [10], the GSI data have focused attention on a region of mass and lifetime where short-lived neutral bosons could exist and yet would not have been observed.

More recently, the production of  $e^+e^-$  pairs by heavy ions in emulsion has been presented [11,12] as evidence for new neutral bosons with masses less than  $10 \text{ MeV}/c^2$  and lifetimes between  $3 \times 10^{-16}$  and  $1.5 \times 10^{-15}$  sec.

In this Letter, we report results from a new electron beam-dump experiment, Fermilab E-774. In an electron beam dump, a neutral  $X_0$  will be produced by a process analogous to bremsstrahlung [13]; it can then be detected by its decay in flight into an  $e^+e^-$  pair provided it does not decay or interact inside the beam dump. If the  $X_0$  decays predominantly into  $e^+e^-$ , its production rate is determined by a single coupling constant which is in turn fixed by the presumed mass and lifetime of the  $X_0$ .

The experiment used an electron beam with 275-GeV/ $c$  mean momentum,  $\pm 6\%$  momentum spread, and 6% hadron contamination. The apparatus (Fig. 1) included a set of beam-defining scintillation counters, a tungsten electromagnetic calorimeter (the electron beam dump), and a pair of scintillation counters immediately behind the dump to veto events in which any charged particles emerged. A second calorimeter with separate electromagnetic and hadronic sections was located 7.25 m downstream from the beam dump. Between the beam dump and the downstream calorimeter, all particles passed through four scintillation counters. The pulse heights recorded in these counters were used to determine the

charge multiplicity of neutral particles decaying in flight. The first of these counters was 2 m downstream from the beam dump and defined the end of the decay space for charged final states. Near the end of the decay space, an additional veto counter with a 5-cm-square hole was used to tag events with wide angle tracks.

Because the bremsstrahlung production spectrum of a particle of mass  $> 2m_e$  is strongly peaked at high secondary energy and small production angle [13], a new particle would cause an excess of events with large energy deposition in the downstream electromagnetic calorimeter, signals corresponding to two charged particles in the decay volume scintillators, and no wide angle tracks.

The experiment trigger required an energy deposition

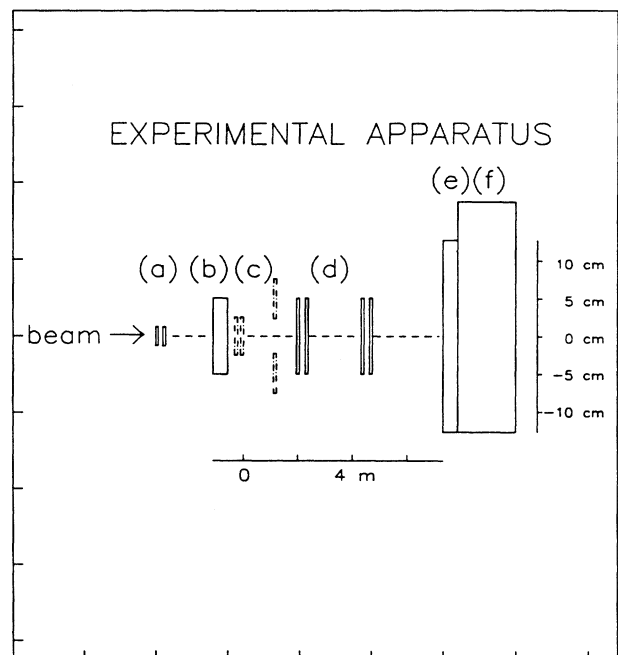


FIG. 1. Layout of experimental apparatus showing (a) beam counters, (b) target calorimeter, (c) veto counters, (d) multiplicity counters, (e) trigger electromagnetic calorimeter, and (f) hadron calorimeter.

in the downstream electromagnetic calorimeter greater than 10% of the nominal beam energy in coincidence with a beam particle and no signal from the veto counters immediately behind the dump. There was no trigger requirement on the signals from the counters in the decay volume, nor on the signals from the target calorimeter or the hadron calorimeter.

Since the beam-dump technique depends on the neutral particle emerging from the dump before it decays, the sensitivity of the experiment was determined largely by the beam energy and the dump length. To maximize the sensitivity to short lifetimes, the target calorimeter was made as short as possible and consisted of two 28-radiation-length-thick stacks of tungsten plates instrumented with scintillating fiber ribbons [14]; the overall target length, including veto counters, was 30 cm. For comparison,  $1.14\text{-MeV}/c^2$  particles with lifetime  $1.3 \times 10^{-15}$  sec as described in Ref. [12] produced at 275 GeV would have an average path length of over 9 cm, and hence a substantial detection probability.

The experiment operated at a typical intensity of  $10^7$  particles per 22-sec beam pulse. The data described here represent  $0.52 \times 10^{10}$  electrons on target, which produced  $1.6 \times 10^5$  triggers. The reduction of these data consisted of three steps: the removal of events caused by multiple beam particles or identifiable hadronic interactions in the target calorimeter, the classification of the remaining events by charge multiplicity, and the separation of the electromagnetic and hadronic final states for each multiplicity.

The first step was accomplished by the following cuts. Events were removed from the data sample if the pulse height in the beam counters indicated more than one beam particle, or if the sum of the calorimeter energies (target, trigger, and hadronic calorimeters) differed from

the mean beam energy by more than 30%. Events in which the energy measurements were distorted by a residual signal from previous interactions were rejected. Finally, to remove most hadron interactions in the target, events were rejected if  $E > 0.04E_{\text{beam}}$  appeared in the second section of the target calorimeter. To determine the inefficiency induced by these cuts, the cuts were also applied to a sample of unbiased beam tracks. Our quoted number of electrons on target has been corrected for this inefficiency.

For events surviving the cuts, we defined the charge multiplicity as the smallest pulse height from among the four decay volume scintillators. The charge multiplicity distribution is shown in Fig. 2(a). Clearly visible are the expected peaks at multiplicity 0 for neutral particles that failed to decay or decayed into neutral final states, and at 2 for neutral particles that decayed into two charged particles. The prominent peak at multiplicity 1 is due to a small inefficiency of the veto counters ( $2 \times 10^{-5}$ ) which allowed beam particles to pass through the apparatus and satisfy the trigger.

Hadronic and electromagnetic final states were distinguished by the fraction of the downstream energy appearing in the hadron calorimeter,  $f_{\text{hadron}}$ . Figures 3(a)–3(c) show the distribution of this fraction for multiplicity 0, 1, and 2 events. The peaks at low  $f_{\text{hadron}}$  in the multiplicity 0 and 2 plots are neutral electromagnetic final states and electromagnetic final states with two charged particles, respectively. The absence of any such peak in the multiplicity 1 plot shows the clear separation between electromagnetic and hadronic final states. The electromagnetic sample is defined by  $f_{\text{hadron}} < 0.16$ . Figure 2(b) shows the multiplicity spectrum for the electromagnetic events. Compared to Fig. 2(a), the multiplicity 1 peak is strongly suppressed.

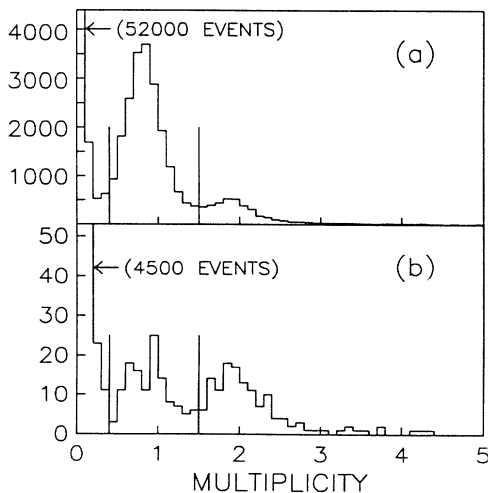


FIG. 2. Distributions in charged multiplicity (a) for all data and (b) for electromagnetic events.

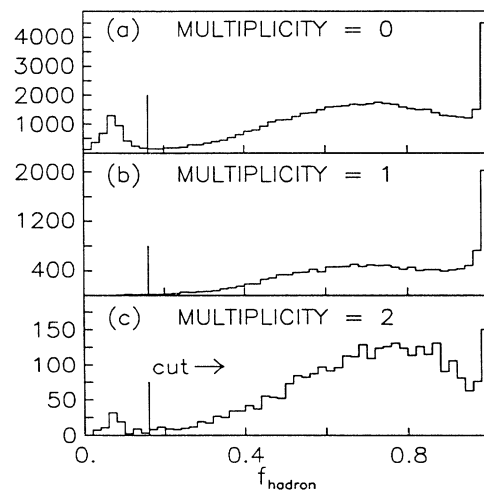


FIG. 3. Distributions in  $f_{\text{hadron}} = E_{\text{hadron}}/E_{\text{em+hadron}}$  for events selected by multiplicity.

Given this sample of identified electromagnetic events, we define a quantity  $x = E_{\text{trigger}}/(E_{\text{trigger}} + E_{\text{target}})$ , where  $E_{\text{trigger}}$  and  $E_{\text{target}}$  are the energies in the trigger and target electromagnetic calorimeters. Figures 4(a) and 4(b) show the  $x$  distributions for charge multiplicity 0 and 2. Any signal for a new particle would appear as an excess of events at large  $x$  in Fig. 4(b). The remaining analysis is concerned with identifying and measuring the contamination from hadronic final-state events and contributions from conventional electromagnetic processes to the spectrum in Fig. 4(b), using the identified hadronic events and the multiplicity 0 (neutral) event spectrum.

There are two corrections to the spectrum in Fig. 4(b) due to purely hadronic events. The first is for multiplicity 1 hadronic events that are doubly misidentified as electromagnetic and multiplicity 2. Though there were few of these events, they typically were at large  $x$  and could thus simulate a real signal. The probability for a single hadron to be mismeasured as multiplicity 2 ( $1.35 \times 10^{-2}$ ) and to be misidentified as electromagnetic ( $2.9 \times 10^{-3}$ ) have both been determined from pion calibration runs. The second correction was for multiplicity 2 hadronic final states, e.g.,  $K_S^0 \rightarrow \pi^+ \pi^-$ , which were misidentified as electromagnetic events. The misidentification probability in this case ( $7.0 \times 10^{-4}$ ) was determined from a Monte Carlo calculation using the measured response to single pions as input. The observed  $x$  distributions for multiplicity 1 and 2 hadrons were normalized to the appropriate misidentification probabilities and used to correct the spectrum of Fig. 4(b). Since the multiplicity 0 electromagnetic spectrum plays a role in the final step of the analysis, it was also corrected for misidentified hadronic events, using the multiplicity 0 hadronic spectrum and assuming that the misidentification probability is the same as for the charged case. The resulting subtractions

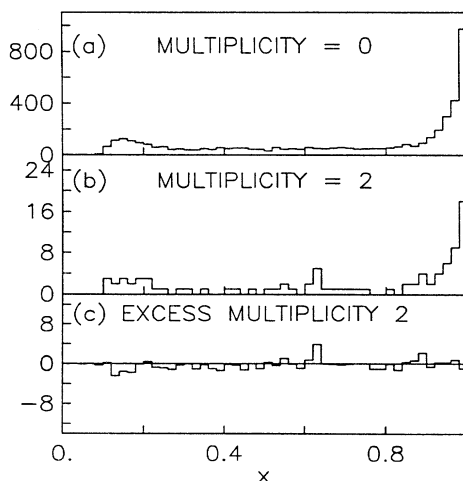


FIG. 4. Distributions in  $x = E_{\text{trigger}}/(E_{\text{trigger}} + E_{\text{target}})$  for electromagnetic events with charged multiplicity 0 and 2, and for excess multiplicity 2 electromagnetic events.

are negligibly small in all but the last few high  $x$  bins of Figs. 4(a) and 4(b), where they range up to 5%.

The final step in the analysis requires some assumption about the nature of the multiplicity 0 electromagnetic events. Clearly, these events consist of photons from the decay of neutral pions, and such events will necessarily contribute to the multiplicity 2 spectrum through conversions and Dalitz pairs. A major known source of these events is the decay  $K_S^0 \rightarrow \pi^0 \pi^0$ , where the  $K_S^0$  was a leading particle produced by a beam  $K^-$ . We have also considered kaons produced by beam pions, which could contribute if the associated strange particle was not detected or was too soft for the event to be classified as hadronic. Another possibility is  $\pi^- p \rightarrow (\pi^0)^n n$ , where the interaction occurs in the last fraction of a radiation length of the target and the photons escape without converting. While calculation suggests that the contribution from this last process is negligible, it is not possible to estimate reliably the admixture of the above processes. We have made the conservative assumption, which leads to the smallest background subtraction, that this set of events consists entirely of isolated  $K_S^0$ . Using this assumption, the background spectrum  $dN_2/dx$  of multiplicity 2 electromagnetic events was calculated directly from the corrected multiplicity 0 electromagnetic spectrum  $dN_0/dx$  using

$$\frac{dN_2}{dx} = \frac{dN_0}{dx} \frac{1 - e^{-l/\gamma c \tau}}{1 - e^{-L/\gamma c \tau}} (2b + 4f),$$

where  $l$  is the distance from the beam dump to the first multiplicity counter,  $L$  is the distance from the beam dump to the trigger calorimeter,  $b$  is the Dalitz decay branching fraction,  $f=0.009$  is the conversion probability for a single photon, and  $\tau$  is the  $K_S^0$  lifetime.

The subtraction of this background from the multiplicity 2 electromagnetic spectrum is shown in Fig. 4(c). There are no excess events within the statistical precision of the plot. Given the 71 events in the unsubtracted spectrum of Fig. 4(b), the 90%-confidence-level upper bound on the number of events with  $x > 0.3$  due to a neutral  $X_0$  is 17 events or  $3.26 \times 10^{-9}$  event per incident electron.

This result constrains the interpretation of the  $e^+e^-$  events seen in emulsions [11,12]. For example, a spin-zero  $X_0$  with mass  $1.14 \text{ MeV}/c^2$  and lifetime  $1.3 \times 10^{-15}$  sec would yield 4700 events in Fig. 4(c) if it decayed primarily to  $e^+e^-$ . Such a particle can therefore exist only if its branching fraction into  $e^+e^-$  is less than 0.06, or its interaction cross section is greater than 120 mb.

Following previous beam-dump experiments [8,9], we have calculated our yield of observed  $e^+e^-$  pairs as a function of mass and lifetime, assuming a unit branching fraction into  $e^+e^-$ . For a spin-0 particle of mass  $1.14 \text{ MeV}/c^2$ , we find that the lifetime must be less than  $4 \times 10^{-16}$  sec or greater than  $4.5 \times 10^{-12}$  sec. Figure 5 shows the regions of mass and lifetime excluded at 90% C.L. assuming pseudoscalar coupling for the hypothetical neutral boson. Longer lifetimes are already ruled out by

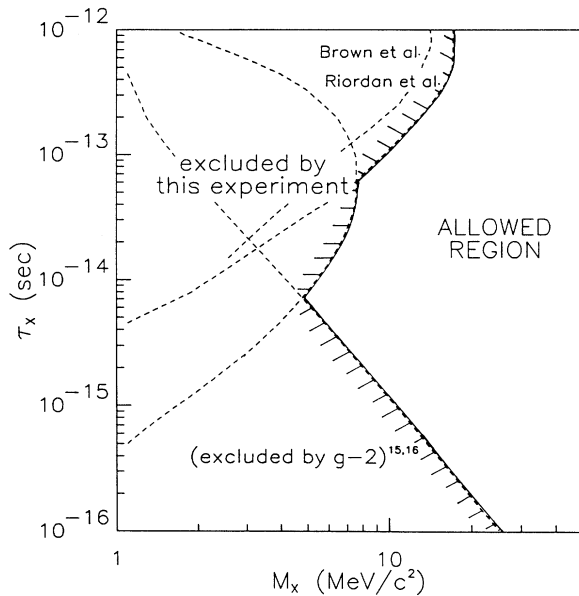


FIG. 5. Mass-lifetime region excluded at 90% C.L. for a pseudoscalar  $X_0$  by this experiment, by Brown *et al.* [8], by Riordan *et al.* [9], and by measurements of  $g-2$  [15,16].

the previous beam-dump experiments. Shorter lifetimes are constrained [4] by bounds obtained from agreement between theory [15] and experiment [16] for the anomalous magnetic moment of the electron ( $g-2$ ). Our data, in conjunction with the  $g-2$  limit, rule out a pseudoscalar particle lighter than  $4.8 \text{ MeV}/c^2$ . We have also considered  $S$ ,  $V$ , and  $A$  couplings, for which the mass limits are 5.0, 4.1, and  $5.8 \text{ MeV}/c^2$ , respectively. These limits are subject to the following provisions. It has been pointed out [4] that bosons of opposite parity contribute to  $g-2$  with opposite signs. Hence, for the case of *more than one new boson*, the  $g-2$  limit could be violated due to cancellation. The interpretation of our data assumes that the  $X_0$  is not a strongly interacting particle. Finally, the case of a spatially extended  $X_0$  has been considered by Schafer [13]. Our limits are not valid for particle radii in excess of 100 fm. For smaller particle radii, a form factor enhances the bremsstrahlung production cross sec-

tion, increasing our sensitivity.

We thank the Fermilab Research Division and the Fermilab Physics Department for their help in construction of the apparatus, and the E-687 Collaboration for sharing the electron beam. This research was supported by the U.S. Department of Energy and the A. P. Sloan Foundation.

<sup>(a)</sup>Now at Fermilab, Batavia, IL 60510.

- [1] J. Schweppe *et al.*, Phys. Rev. Lett. **51**, 2261 (1983); M. Clemente *et al.*, Phys. Lett. **137B**, 41 (1984); T. Cowan *et al.*, Phys. Rev. Lett. **54**, 1761 (1985).
- [2] A. Schafer *et al.*, J. Phys. G **11**, L69 (1985); A. B. Balantekin *et al.*, Phys. Rev. Lett. **55**, 461 (1985); N. C. Mukhopadhyay and A. Zhender, Phys. Rev. Lett. **56**, 206 (1986).
- [3] T. Cowan *et al.*, Phys. Rev. Lett. **56**, 444 (1986).
- [4] J. Reinhardt *et al.*, Phys. Rev. C **33**, 194 (1986).
- [5] A. Schafer *et al.*, Mod. Phys. Lett. A **1**, 1 (1986).
- [6] M. J. Savage *et al.*, Phys. Rev. Lett. **57**, 178 (1986); A. J. Hallin *et al.*, Phys. Rev. Lett. **57**, 2105 (1986).
- [7] A. Konaka *et al.*, Phys. Rev. Lett. **57**, 659 (1986).
- [8] C. N. Brown *et al.*, Phys. Rev. Lett. **57**, 2101 (1986).
- [9] E. M. Riordan *et al.*, Phys. Rev. Lett. **59**, 755 (1987).
- [10] U. von Wimmersperg *et al.*, Phys. Rev. Lett. **59**, 266 (1987); K. Maier *et al.*, Z. Phys. A **326**, 527 (1987); J. van Klinken *et al.*, Phys. Lett. B **205**, 223 (1988); E. Lorenz *et al.*, Phys. Lett. B **214**, 10 (1988); H. Tsertos *et al.*, Phys. Rev. D **40**, 1397 (1989).
- [11] M. El-Nadi and O. E. Badawy, Phys. Rev. Lett. **61**, 1271 (1988).
- [12] F. W. N. de Boer and R. van Dantzig, Phys. Rev. Lett. **61**, 1274 (1988).
- [13] Y. S. Tsai, Phys. Rev. D **34**, 1326 (1986); A. Schafer, Phys. Lett. B **211**, 207 (1988); Y. S. Tsai, SLAC Report No. SLAC-PUB-4877, 1989 (unpublished).
- [14] A. Bross *et al.*, Nucl. Instrum. Methods Phys. Res., Sect. A **286**, 69-72 (1990).
- [15] T. Kinoshita, in *Proceedings of the 1986 Conference on Precision Electromagnetic Measurements, Gaithersburg, Maryland, 1986*, edited by R. F. Dzuba (IEEE, New York, 1986).
- [16] R. S. Van Dyck, Phys. Rev. Lett. **38**, 310 (1977).